An alternative force state map for shock absorbers

S Duym
Department of Electrical Engineering, Vrije Universiteit Brussel, Brussels, Belgium

Abstract: Automotive shock absorbers are commonly characterized by their force–velocity diagram. Nevertheless, mainly due to gas entrapped in the damper fluid, hysteretic effects can be observed on the characteristic curve. In order to improve the accuracy of the description and possible simulations, the restoring force method was used to describe the damper force. According to the restoring force method or equivalent force state mapping technique, the damper force is fitted as a non-parametric function of both velocity and displacement. However, it is shown for a damper under test that a more appropriate choice would be to use velocity and acceleration as independent variables instead of displacement and velocity for broadband excitation signals.

Keywords: non-linear dynamics, non-parametric modelling, automotive shock absorbers

1 INTRODUCTION

Shock absorbers and springs form the vital parts of a car suspension. The suspension of a vehicle is responsible for the ride comfort and the stability pertaining to driving. Therefore, it is important to tune the shock absorber and the spring relative to the modal behaviour of the car body so as to avoid the enhanced effect of unwanted resonances. In the past, attempts have been made to predict the dynamical behaviour of a car by simulation, but the primary simulation results showed poor correlation with the actual measurements. This was due to the fact that the dampers were modelled as pure linear elements. Today the linear modelling of a shock absorber has been rejected and replaced by a two-slope or three-slope model which represents the most important non-linearity in the characteristic diagram. Unfortunately, the characteristic diagram of some dampers can also exhibit a rather strong hysteresis. The damper type tested in this paper is normally used on the front suspension of a Porsche. This choice was made because this type is notorious among commercial dampers for its significant hysteretic effects. The characteristic diagram of the absorber is shown in Fig. 1. A significant hysteresis can falsify the simulation results obtained from a simple two-slope model.

One of the most complete models described in the literature is the physical model of Lang (**1**). This iterative model takes into account the hysteresis due to the compliance of the cylinder walls, the compressibility of the fluid and the occurrence of a vapour or gas phase. However, the model requires the knowledge of more than 80 parameters and was originally implemented using an analogue computer. The identification of the coefficients is hampered by their strong intercorrelations and the iterative character of Lang's model slows down the potential identification considerably.

With the introduction of the restoring force method, an attempt was made to identify non-parametrically the damper force as a function of displacement and velocity (**2**). Unlike most damper models, this model enables a fast (non-iterative) and easy identification since the non-linear model is linear in the parameters. The choice of displacement as the independent variable is supported by the apparent stiffness due to the compressibility of the mixed air/oil solution. Nevertheless, further experiments showed

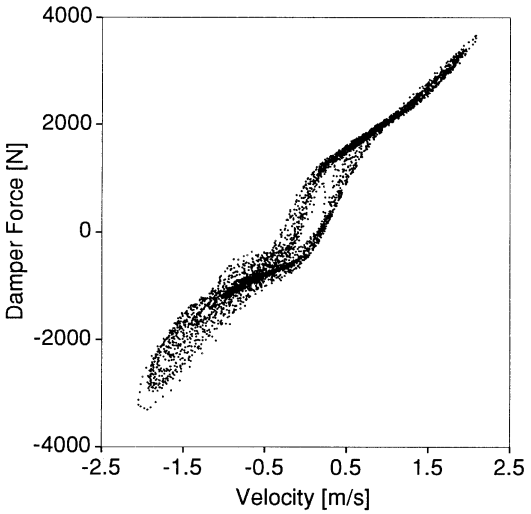

Fig. 1 Characteristic diagram of the damper under test

The MS was received on 20 October 1995 and was accepted for publication on 14 May 1996.

that this did not produce adequate models except for unifrequent excitation, hence the use of 'isofrequent maps' (**3**). The use of 'difference surfaces' proved the frequency dependency, but also indicated that this was not just caused by inertia effects. The use of isofrequent maps is rather limited since they are no longer valid for broadband excitation such as the classic random noise. Besides the frequency dependency the damper force is also sensitive to the viscosity which is temperature dependent. Consequently, if the damper is to be modelled with the restoring force model, it is possible to end up with a large collection of maps (**4**). Most models consider a constant temperature condition.

2 THEORY

With the local restoring force method a combination of the original restoring force method and the equivalent force state mapping was presented (**5**). Basically, it divides the state plane, built up from velocity and displacement, into regular grid elements (p, q). A Taylor expansion truncated at order r is written out for each grid element to which the data in the considered element are fitted [see equation (1)]. Each measurement sample delivers a quadruplet (x_i^{pq}, $\dot{x}_i^{pq}$, $\ddot{x}_i^{pq}$, g_i^{pq}) respectively displacement, velocity, acceleration and damper force. The alternative model uses acceleration as the independent variable instead of displacement. The model is formulated in an analogous manner [see equation (2)] and n_1 and n_2 are the number of bin elements of the two respective independent variables. The coefficients c_{t_1,t_2}^{pq} are recovered using a least-squares estimator.

Model 1: $g(\dot{x}_i^{pq}, x_i^{pq})$

$$g(\dot{x}_i^{pq}, x_i^{pq}) = \sum_{t_1=0}^{r} \sum_{t_2=0}^{r-t_1} c_{t_1 t_2}^{pq} (\dot{x}_i^{pq})^{t_1} (x_i^{pq})^{t_2}$$

for all grid elements $p = 1, \ldots, n_1$ and $q = 1, \ldots, n_2$ (1)

Model 2: $g(\dot{x}_i^{pq}, \ddot{x}_i^{pq})$

$$g(\dot{x}_i^{pq}, \ddot{x}_i^{pq}) = \sum_{t_1=0}^{r} \sum_{t_2=0}^{r-t_1} c_{t_1 t_2}^{pq} (\dot{x}_i^{pq})^{t_1} (\ddot{x}_i^{pq})^{t_2}$$

for all grid elements $p = 1, \ldots, n_1$ and $q = 1, \ldots, n_2$ (2)

In order to qualify both models the root mean square (r.m.s.) value is calculated according to equation (3). This is the root of a classic least-squares cost. N is the total number of measurement samples and n_{pq} is the number of samples associated with grid cell (p, q).

$$k = \sqrt{\left\{ \frac{1}{N} \sum_{p=1}^{n_1} \sum_{q=1}^{n_2} \sum_{i=1}^{n_{pq}} [g_i^{pq} - g(\dot{x}_i^{pq}, x_i^{pq} \text{ or } \ddot{x}_i^{pq})]^2 \right\}} \quad (3)$$

3 EXPERIMENTAL RESULTS

A similar test set-up was used to that described in reference (**2**). The only difference was that displacement and velocity were measured and acceleration was derived numerically from velocity in this study. The data were sampled at 1000 Hz. Low-pass filters with a cut-off frequency of 300 Hz were used to avoid aliasing. Supplementary digital low-pass filtering from 250 Hz was performed directly in frequency domain (DFT) to avoid the amplification of high-frequency noise during differentiation of velocity (**6**).

In reference (**2**) the data were obtained from 87 sinusoidal sequences. In order to guarantee a minimum change in temperature, the excitation time should be as short as possible. In this study, this was realized with the use of specially designed periodic signals (**7**). These signals, referred to as multisines, also make it possible to estimate the amount of measurement noise. Another important advantage of using periodic signals is that filtering and differentiation are exact operations (**6**). In Fig. 2, the time history of the displacement for one period is displayed. The amplitude spectrum was designed to simulate the effect of car and wheel resonances. The spectrum contains 16 sines with frequencies from 1.25 to 16.25 Hz. The phase spectrum was optimized with the procedure given in reference (**7**) so as to produce a uniform state plane covering, as shown in Fig. 3a. The alternative covering is worse but still satisfactory (Fig. 3b).

In Table 1, the r.m.s. values for models 1 and 2 are given for four different grid distributions with a constant number of cells ($n_1 n_2 = 128$). For each case a zero- ($r = 0$) and

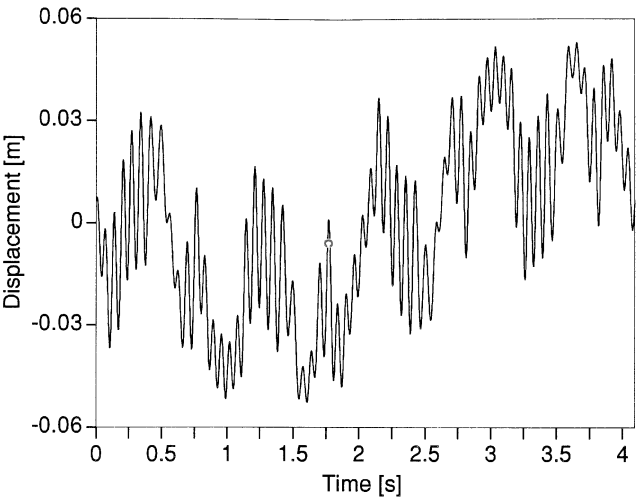

Fig. 2 Displacement history of one period

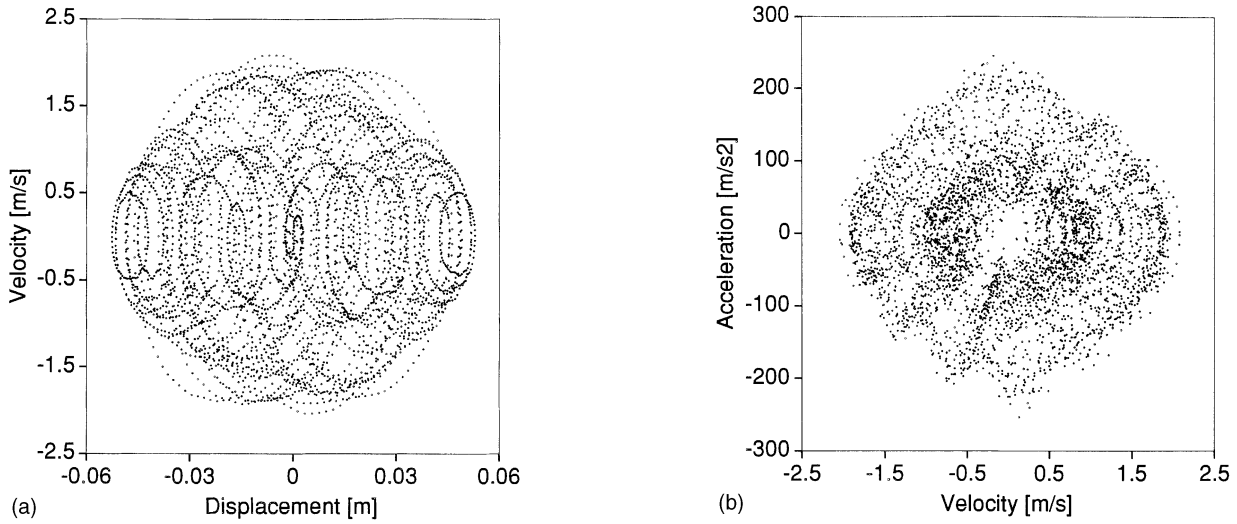

Fig. 3 State plane for (a) displacement–velocity and (b) velocity–acceleration

Table 1 Root mean square error for broadband multisine (1.25–16.25 Hz) in steps of 1 Hz

k (N)		$g(\dot{x}_i^{pq}, x_i^{pq})$ map		$g(\dot{x}_i^{pq}, \ddot{x}_i^{pq})$ map	
n_1	n_2	$r = 0$	$r = 1$	$r = 0$	$r = 1$
4	32	484.0	225.9	427.6	106.4
8	16	327.1	219.3	246.3	68.9
16	8	256.4	220.1	147.1	59.5
32	4	237.4	222.3	118.2	60.0

first- ($r = 1$) order model is fitted. It is clear that the best model is given for the alternative model (model 2) with a 16 by 8 grid. Compared to the standard deviation of the measurement noise, which is 32.4 N per sample, the new model (model 2) performs satisfactorily in contrast to the former model (model 1). The model error can be reduced by increasing the number of grid elements. In addition, it is possible to find an optimal distribution for a given number of grid cells that minimizes the total error. More details are given in reference (**8**). In Fig. 4, two first-order maps are shown for each model for a grid of 16 by 8 elements. A clear trend in the function of acceleration (Fig. 4b) can be detected in contrast with the classic force state map (Fig. 4a). Figure 5 gives an idea how both models perform in reconstructing the damper force.

In a second experiment a beating signal was applied to the shaker. The beating signal was the superposition of two sinusoids with nearly equal frequencies (**6**). The amplitudes were chosen equal to each other but a phase shift of 180° was used. In Table 2 the results for the fit on the second

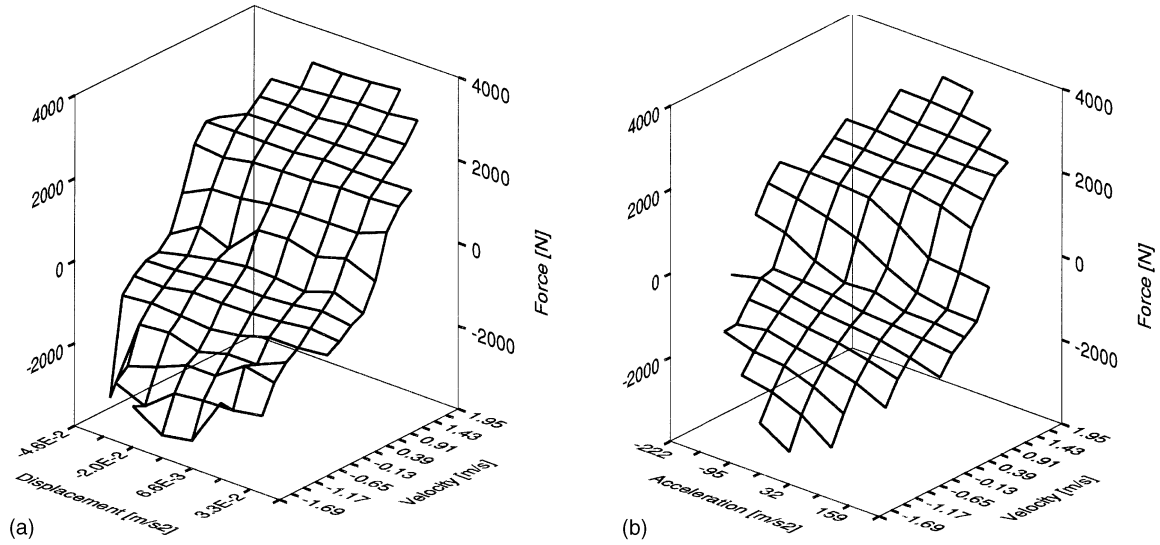

Fig. 4 First-order force state map for a 16 by 8 grid for (a) displacement–velocity and (b) velocity–acceleration

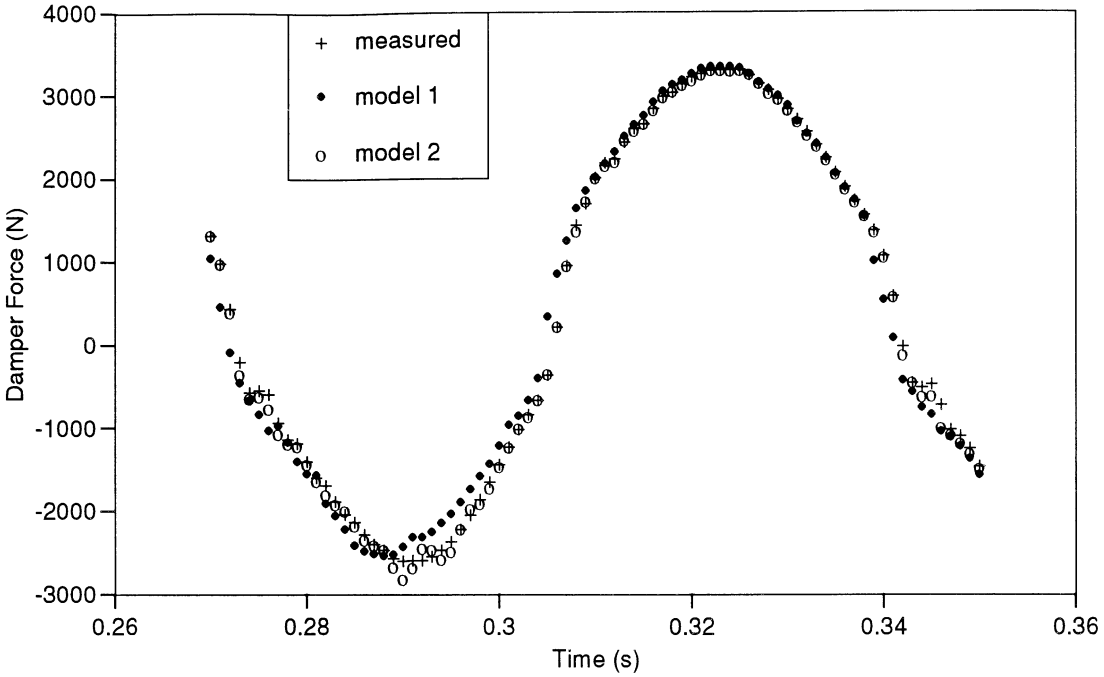

Fig. 5 Damper force versus time; measured and reconstructed from both models (detail)

Table 2 Root mean square error for beating signal (5.0–5.2 Hz)

k (N)		$g(\dot{x}_i^{pq}, x_i^{pq})$ map		$g(\dot{x}_i^{pq}, \ddot{x}_i^{pq})$ map	
n_1	n_2	$r = 0$	$r = 1$	$r = 0$	$r = 1$
4	32	396.0	114.6	397.2	125.7
8	16	255.7	60.5	254.0	59.2
16	8	137.0	28.6	140.1	36.5
32	4	96.2	26.6	106.3	35.9

experiment are shown. This time no relevant differences can be detected and the classical restoring force model is found to perform even somewhat better than the alternative. Since a beating signal is almost unifrequent, this result is not surprising. Because of its small bandwidth the displacement appears to be proportional to acceleration [see equation (4)]. This explains why the force data obtained from a beating signal can be properly fitted with the classical method.

$$\ddot{x} \cong -(2\pi f)^2 x \tag{4}$$

with f the centre frequency. Other dampers were tested and the same kind of results were observed although the quality did not improve that much because of smaller hysteretic effects.

4 CONCLUSIONS

The damper force of a specified damper with important hysteretic effects is characterized as a non-parametric function of two state variables. Besides the first variable velocity, the choice of the second variable, displacement or acceleration, can influence the quality of the model. For harmonic or nearly unifrequent excitation, the fit quality is comparable for both alternatives. However, for broadband excitation, the choice of acceleration instead of displacement as second variable clearly improves the quality of the model. For more accurate simulation results with a fast and easily identifiable model, the new alternative model can be considered for automotive shock absorbers.

ACKNOWLEDGEMENTS

This research is supported by a grant from the Flemish Institute for the Improvement of Scientific and Technological Research in Industry (IWT), the Belgian National Fund for Scientific Research (NFWO), the Flemish government (GOA-IMMI$_2$) and the Belgian government as a part of the Belgian programme on InterUniversity Poles of Attraction (IUAP-50) initiated by the Belgian State, Prime Minister's Office, Science Policy Programming. The measurements took place in the Research Laboratories of Monroe Europe, at St Truiden, Belgium. The author wishes to express his gratitude to the Monroe personnel for their assistance, especially K. Reybrouck and H. Geukens.

REFERENCES

1 **Lang, H. H.** A study of the characteristics of automotive hydraulic dampers at high stroking frequencies. PhD thesis, University of Michigan, 1977.
2 **Belingardi, G.** and **Campanile, P.** Improvement of the shock

absorber dynamic simulation by the restoring force mapping method. 15th International Seminar on *Modal Analysis*, Heverlee, Belgium, 1990, pp. 441–454.

3 Worden, K. and **Tomlinson, G. R.** Parametric and nonparametric identification of automotive shock absorbers. 10th International Conference on *Modal Analysis*, San Diego, California, 1992, pp. 764–771.

4 Surace, C., Storer, D. and **Tomlinson, G. R.** Characterising an automotive shock absorber and the dependency on the temperature. 10th International Conference on *Modal Analysis*, San Diego, California, 1992, pp. 1317–1326.

5 Duym, S., Schoukens, J. and **Guillaume, P.** A local restoring force surface method. 13th International Conference on *Modal Analysis*, Nashville, Tennessee, 1995, pp. 1392–1399.

6 Worden, K. Data processing and experiment design for the restoring force surface method. *Mech. Systems and Signal Processing*, 1990, **4**(4), 295–344.

7 Duym, S. and **Schoukens, J.** Design of excitation signals for the restoring force surface method. *Mech. Systems and Signal Processing*, 1995, **9**(2), 139–158.

8 Duym, S. and **Schoukens, J.** On selecting an optimal force-state map. International Conference on *Identification in Engineering Systems*, Swansea, United Kingdom, 1996, pp. 446–455.